Hypoxia-Induced Scleral HIF-2α Upregulation Contributes to Rises in MMP-2 Expression and Myopia Development in Mice

Wenjing Wu,[1,2] Yongchao Su,[1,2] Changxi Hu,[1,2] Huixin Tao,[1,2] Ying Jiang,[1,2] Guandong Zhu,[1,2] Jiadi Zhu,[1,2] Ying Zhai,[1,2] Jia Qu,[1–3,5] Xiangtian Zhou,[1–5] and Fei Zhao[1–2]

[1]School of Ophthalmology and Optometry and Eye Hospital, Wenzhou Medical University, Wenzhou, Zhejiang, China
[2]State Key Laboratory of Optometry, Ophthalmology, and Vision Science, Wenzhou, Zhejiang, China
[3]National Clinical Research Center for Ocular Diseases, Wenzhou, Zhejiang, China
[4]Research Unit of Myopia Basic Research and Clinical Prevention and Control, Chinese Academy of Medical Sciences (2019RU025), Wenzhou, Zhejiang, China
[5]Oujiang Laboratory, Wenzhou, Zhejiang, China

Correspondence: Fei Zhao, School of Ophthalmology and Optometry and Eye Hospital, Wenzhou Medical University, 270 Xueyuan Road, Wenzhou, Zhejiang 325027, China; zhaofei@eye.ac.cn.
Xiangtian Zhou, School of Ophthalmology and Optometry and Eye Hospital, Wenzhou Medical University, 270 Xueyuan Road, Wenzhou, Zhejiang 325027, China; zxt@mail.eye.ac.cn.

WW and YS contributed equally to this work.

Received: April 20, 2022
Accepted: June 15, 2022
Published: July 8, 2022

Citation: Wu W, Su Y, Hu C, et al. Hypoxia-induced scleral HIF-2α upregulation contributes to rises in MMP-2 expression and myopia development in mice. *Invest Ophthalmol Vis Sci.* 2022;63(8):2. https://doi.org/10.1167/iovs.63.8.2

Purpose. Scleral hypoxia is a key factor that induces hypoxia-inducible factor-1α (HIF-1α) upregulation, and this response contributes to myopia progression. Currently, we aim to determine if the different HIF subtypes, including HIF-1α and HIF-2α, mediate hypoxia-induced myopia development through promoting scleral MMP-2 expression and collagen degradation.

Methods. Our study included: (1) time-course of scleral HIF-2α, MMP-2, and COL1α1 expression during form-deprivation myopia (FDM) development was determined in C57BL/6J mice. (2) The effect of silencing either HIF-1A or HIF-2A on hypoxia-induced alterations in MMP-2 expression was analyzed in cultured human scleral fibroblasts (HSFs) under a hypoxic condition (i.e. 1% oxygen). (3) To knock-down either HIF-1α or HIF-2α expression in the sclera, we performed Sub-Tenon's capsule injection of an adeno-associated virus (AAV)8-packaged Cre overexpression vector (AAV8-Cre) in *HIF-1α*$^{fl/fl}$ or *HIF-2α*$^{fl/fl}$ mice. HIF-1α, HIF-2α, MMP-2, and COL1α1 expression were analyzed by Western blot or quantitative real-time PCR (qRT-PCR). In addition, the effects of scleral HIF-2α knock-down on normal refractive development and FDM development were evaluated.

Results. The time-dependent increases in scleral HIF-2α mimicked the HIF-1α expression profiles as we previously described. Hypoxia significantly promoted MMP-2 expression in HSFs, and this upregulation was solely alleviated by HIF-2A rather than HIF-1A silencing. Scleral HIF-2α knockdown significantly inhibited form-deprivation (FD)-induced MMP-2 upregulation and declines in COL1α1 accumulation and myopia development. Although scleral HIF-1α knockdown also significantly suppressed FD-induced declines in COL1α1 accumulation, it did not abrogate scleral MMP-2 upregulation.

Conclusions. HIF-2α rather than HIF-1α induces myopia development through upregulating MMP-2 and promoting collagen degradation in the sclera.

Keywords: hypoxia, hypoxia-inducible factor (HIF), collagen, matrix metalloproteinase (MMP), myopia, sclera

Myopia is currently the most prevalent refractive error worldwide that can lead to severe visual impairment.[1] Its incidence is reaching epidemic proportions, especially in Southeast and East Asia.[2] By 2050, the world prevalence of myopia and high myopia (refraction ≥ −6.00 diopters [D]) is predicted to increase to 49.8% and 9.8%, respectively.[3] The high myopia often leads to a variety of sight-threatening complications, such as cataract, retinal detachment, macular hole, peripapillary deformation, choroidal neovascularization, and glaucoma.[4] Even though significant advances have been made in treating this condition, the procedures have limitations. Therefore, there is still a need to develop novel therapeutic options to improve management of this condition. Satisfying this objective depends on obtaining the necessary insight to identify novel targets for selectively improving therapeutic management of this condition.

Most of human myopia is characterized by excessive ocular elongation of both the vitreous chamber depth (VCD) and axial length (AL). In order to accommodate the inappropriate optical axis elongation, the scleral thickness decreases which increases its extensibility. This thinning process occurs as a consequence of decreases in collagen accumulation that are due to the combined effects of decelerated synthesis and accelerated degradation of the

collagen framework and alteration of extracellular matrix (ECM) components.[5] Homeostatic control of eye growth is dependent on the control of collagen accumulation and scleral ECM remodeling.[6] Type I collagen is the major ECM component, which constitutes approximately 90% of the scleral dry weight. Distinct subtypes of proteases are known to mediate ECM degradation and scleral thinning.[7] Matrix metalloproteinase type 2 (MMP-2) is one of the enzymes that undergoes upregulation during this process.[8] In addition, it was shown in a mice model that MMP-2 knockdown significantly suppressed the decreases in scleral alpha 1 chain of type I collagen (COL1α1) accumulation during myopia.[9] Furthermore, fibroblasts are the major scleral cell type and they along with monocyte-derived macrophages, which migrate into the sclera from the circulation, are the primary sources of MMP-2 upregulation. Their contributions to MMP-2 upregulation were confirmed based on showing that either fibroblast or macrophage- specific *Mmp-2* deletion alleviated myopia development in mice.[9,10] However, the identity of the mediators that promote MMP-2 upregulation in the different cell types require clarification.

Scleral hypoxia is a prominent regulatory candidate factor which induces myopia development in both different animal models and humans.[11,12] This is evident because the administration of either salidroside or formononetin, which are the anti-hypoxic drugs to guinea pigs, inhibited myopia development.[11] Under both physiological and pathological conditions, hypoxia increased the expression levels of MMP-2 and some other MMP family members.[13–16] Conversely, hypoxia also decreased the expression levels of MMPs in different conditions.[17,18] However, it is unknown if scleral hypoxia mediates MMP-2 upregulation during myopia development.

Hypoxia-inducible factors (HIFs), especially HIF-1α and HIF-2α, are the master regulators of cellular adaptation to hypoxia.[14,19] They play overlapping or distinct roles in ECM remodeling under physiological and pathological conditions.[20,21] HIF-1α involvement in myopia is apparent because it undergoes upregulation during myopia progression in the mouse, guinea pig, and the rabbit models.[11,22] In addition, both the pharmacological inhibition of scleral HIF-1α in guinea pigs[11] and genetic knock-down of scleral HIF-1α in mice[12] suppressed the declines in collagen accumulation and myopia development. Besides, scleral HIF-1α knockdown shifted the refraction toward hyperopia in mice.[12] Moreover, scleral HIF-1α is suggested to be a prominent regulatory candidate for mediating genetic and environmental interactions in human myopia pathogenesis.[12] However, it is unknown if the effects of scleral HIF-2α mirror those of HIF-1α in mediating ECM remodeling and myopia development.

Here, we first evaluated the interdependence between changes in HIF-2α and MMP-2 expression levels and myopia progression in mice. Then, we determined if hypoxia upregulated MMP-2 expression in cultured human scleral fibroblasts (HSFs). In parallel, we assessed if either HIF-1A or HIF-2A knockdown antagonized the effect of hypoxia on MMP-2 expression in HSFs. Finally, we determined if either HIF-1A or HIF-2A knockdown in the sclera suppressed the scleral MMP-2 upregulation and myopia development in mice.

Materials and Methods

Mice

All mice were bred in the animal breeding unit at Wenzhou Medical University (Wenzhou, China) and raised in standard mouse cages at 22 ± 2°C with a 12-hour light/12-hour dark cycle. The lights were turned on at 8:30 AM every day. During the light phase, the luminance was approximately 100 to 200 lux. All animal experiments were approved by the Animal Care and Ethics Committee at Wenzhou Medical University (Wenzhou, China) and conducted according to the Association for Research in Vision and Ophthalmology Statement for the Use of Animals in Ophthalmic and Visual Research.

Generation of Scleral HIF-1α or HIF-2α Knockdown Mice

Hif-1α$^{fl/fl}$ (C57BL/6J background, B6.129-*Hif-1α*^{tm3Rsjo}/J, stock no.: 007561, The Jackson Laboratory, Bar Harbor, ME, USA) or *Hif-2α*$^{fl/fl}$ (C57BL/6J background, *Epas1*^{tm1Mcs}/J, stock no.: 008407, The Jackson Laboratory) mice were subjected to sub-Tenon's capsule injection of an AAV8-Cre virus. The *Hif-1α*$^{fl/fl}$ and *Hif-2α*$^{fl/fl}$ mice injected with AAV8-packaged empty vector (AAV8-vector) served as the control. AAV8s injection was administered as previously described.[9]

Induction of Monocular Form-Deprivation Myopia in Mice and Ocular Biometric Measurements

Monocular form-deprivation myopia (FDM) was induced by occluding the right eye with a translucent occluder, as previously described.[23] Ocular refraction was measured by using an eccentric infrared photorefractor in a dark room, as described in detail previously.[23] Ocular biometric parameters, including VCD and AL, were measured using a custom-made optical coherence tomography (OCT) apparatus, as described in detail previously.[24] Each measurement was repeated three times to obtain a final mean value.

Animal Experimental Paradigms

Scleral HIF-2α, MMP-2, and COL1α1 expression levels during myopia progression were measured in 4-week-old wild-type C57BL/6J male mice (interocular refraction difference, <3.00 D). The animals were randomly divided into two groups. In one group, the right eyes of mice were form deprived for 2 days, 1 week, or 2 weeks (labeled as FD-T), and the untreated left eyes constituted the fellow eye control group (designated FD-F). Mice in the other group were untreated and served as age matched normal controls (designated NC). At these time points, the scleral tissues were isolated and prepared for Western blot analysis.

Effects of scleral HIF-2α knockdown on normal refractive development were evaluated in 4-week-old *Hif-2α*$^{fl/fl}$ mice. Both male and female *Hif-2α*$^{fl/fl}$ mice were assigned to two groups: (1) sub-Tenon's capsule injection of AAV8-Cre; and (2) injection of AAV8-vector control. Ocular measurements were carried out at baseline, and at 2 and 4 weeks after the injections (i.e. when the mice were 4, 6, and 8 weeks old). The scleral tissues obtained from these mice were prepared for qRT-PCR analysis of HIF-2α, Western blot analysis of HIF-2α, HIF-1α, MMP-2, and COL1α1 expression. The retinal and corneal tissues obtained from these mice were prepared for qRT-PCR analysis of HIF-2α. Effects of scleral HIF-2α knockdown on myopia development were evaluated in 4-week-old *Hif-2α*$^{fl/fl}$ mice. These mice were assigned to two groups: (1) AAV8-Cre injection plus FD (AAV8-Cre + FD); and (2) AAV8-vector injection plus FD (AAV8-vector + FD). FD was initiated 1 week after the injections and continued for

Investigative Ophthalmology & Visual Science

the subsequent 2 weeks. Refraction and ocular biometric parameters were measured at baseline, and at 2 weeks after FD (i.e. when the mice were 5 and 7 weeks old). The scleral tissues obtained from these mice were prepared for Western blot analysis of HIF-2α, HIF-1α, MMP-2, and COL1α1 expression.

Effects of scleral HIF-1α knockdown on FD-induced MMP-2 upregulation were evaluated in 4-week-old *Hif-1α*$^{fl/fl}$ mice. These mice were assigned to two groups: (1) AAV8-Cre injection plus FD (AAV8-Cre+FD); (2) AAV8-vector injection plus FD (AAV8-vector + FD). FD was initiated 1 week after the injections and continued for the subsequent 2 weeks. Refraction and ocular biometric parameters were measured at baseline, and at 2 weeks after FD (i.e. when the mice were 5 and 7 weeks old). The scleral tissues obtained from these mice were prepared for Western blot analysis of HIF-1α, HIF-2α, MMP-2, and COL1α1 expression.

Mice were randomly assigned to experimental groups. For experiments using the transgenic mice, both male and female mice were randomly assigned into different groups within each genotype.

Experimental Hypoxia in Cultured HSFs

To explore the potential role of hypoxia on MMP-2 expression, we established cultures of HSFs, as previously described.[25] The cells were grown in Dulbecco's Modified Eagle's Medium (DMEM, 12430, Gibco) supplemented with 10% fetal bovine serum (FBS) and 2 mM GlutaMAX (Gibco) at 37°C in a 5% CO_2 humidified incubator. Cells were seeded in 12-well culture plates at a density of 2.5×10^5 for 24 hours, after which the HSFs were subjected to hypoxic treatments. Hypoxic incubation was performed in a Coy In Vitro Hypoxic Cabinet System (Coy Laboratory Products, Grass Lake, MI, USA) that maintained 1% O_2 for 4, 8, 12, or 24 hours. Cells incubated under normoxia (21% O_2) served as controls.

We then investigated the role of either HIF-1A or HIF-2A knockdown on the effect of hypoxia-induced changes on MMP-2 expression. Silencing RNAs (siRNAs) targeting human *Hif-1α* (target sequences of siRNA-1 and 2: 5′-CAAAGUUCACCUGAGCCUA-3′, and 5′-GAUUAACUCAGUUUGAACU-3′) and *Hif-2α* (target of siRNA-1 and 2: 5′-GCAAAUGUACCCAAUGAUA-3′, and 5′-CGCAAAUGUACCCAAUGAU-3′), and a scrambled-sequence normal control siRNA (NC), were purchased from Sigma-Aldrich. HSFs were seeded in 12-well plate culture dishes. After becoming 60% to 80% confluent, the cells were transfected with siRNAs (final concentration 30 nM) using Lipofectamine RNAiMAX reagent (LipoRNAiMax, Invitrogen) according to the manufacturer's instructions. This was followed by 24 hours of incubation under hypoxic (1% O_2) treatment or normoxic control conditions.

At the end of the designated periods, Western blot analysis determined the HIF-1A, HIF-2A, and MMP-2 protein expression levels.

Tissue RNA Extraction, cDNA Preparation, and Quantitative Real-Time PCR

After the different treatment periods, the mice were euthanized and their eyes were removed. The scleras, retinas, and corneas were collected by dissection. Scleras and corneas were homogenized separately in a ball mill. Total RNA was extracted using the RNeasy Fibrous Tissue Mini Kit (Qiagen, Hilden, Germany), according to the manufacturer's instructions. The total retinal RNA was extracted using TRIZOL reagent (Invitrogen, Carlsbad, CA, USA) according to the manufacturer's protocol. After treatment with RQ1 RNase-Free DNase (Promega, Madison, WI, USA), the RNAs were reverse-transcribed, using random primers and M-MLV reverse transcriptase (Promega) to synthesize cDNA. The qRT-PCR was performed using specific primers and the Power SYBR Green PCR Master Mix (Applied Biosystems, Foster City, CA, USA) on an ABI ViiA 7 Real-Time PCR system (Applied Biosystems). The expression level of *Hif-2α* mRNA, relative to that of 18S rRNA, was determined using threshold cycle values and the $2^{-\Delta\Delta Ct}$ method.[26] The primer sequences are provided in the Table.

Immunoblot Analysis

The mice were euthanized and their eyes were removed after the different treatment periods. Their scleras were collected by dissection and homogenized separately with a ball mill in RadioImmunoPrecipitation Assay buffer (RIPA Lysis Buffer, Beyotime Biotechnology, Shanghai, China) supplemented with 1 mM phenylmethanesulfonyl fluoride (PMSF; Beyotime Biotechnology) and a protease inhibitor cocktail (Roche, Grenzach-Wyhlen, Germany). HSFs were homogenized in the same lysis buffer. The homogenate was further lysed on ice by sonication for about 30 to 60 seconds for complete tissue lysis. After being centrifuged at 13,000 × g for 10 minutes at 4°C, the supernatant was collected. The protein concentration was determined using an Enhanced BCA Protein Assay Kit (Beyotime Biotechnology).

Equal amounts (15 µg) of total protein from HSFs or 30 µg of total protein from mouse scleral samples, were loaded onto a 10% sodium dodecyl sulfate-polyacrylamide gel, separated by electrophoresis, and then blotted onto a nitrocellulose membrane (Millipore, Billerica, MA, USA). After blocking with 5% non-fat milk for 2 hours at room temperature, the membranes were incubated overnight at

Table. Primers for qRT-PCR and Genotype Identification

	Forward Primer	Reverse Primer
Primers for qRT-PCR		
18s	5′-CGGACACGGACAGGATTGAC-3′	5′-GTTCAAGCTGCCCGTCTCCTCATC-3′
Hif-2α	5′- AGTTGCCCCTGCCTCACAGTGT -3′	5′-GGAGCTTATGTGTCCGAAGGAA -3′
Primers for genotype identification of *Hif-1α*$^{fl/fl}$		
	5′-TGCATGTGTATGGGTGTTTTG-3′	5′-GAAAACTGTCTGTAACTTCATTTCC-3′
Primers for genotype identification of *Hif-2α*$^{fl/fl}$		
	5′- GAGAGCAGCTTCTCCTGGAA-3′	5′- TGTAGGCAAGGAAACCAAGG-3′

Investigative Ophthalmology & Visual Science

4°C with primary antibodies against HIF-2α (1:1000; Cat. #ab199; Abcam, Cambridge, MA, USA), HIF-1α (1:800, Cat. #610958; BD Bioscience, San Diego, CA, USA), COL1α1 (1:1000, Cat. #67288; Proteintech Group, Inc, Rosemont, PA, USA), MMP-2 (1:1000, Cat. #10373; Proteintech Group, Inc.), β-actin (1:1000, Cat. #66009; Proteintech Group, Inc.), or α-tubulin (1:2000, Cat. #ab52866; Abcam, Cambridge, MA). After rinsing the membranes 3 times for 5 minutes each with Tris-buffered saline-Tween 20 (TBST, 10 mM Tris-HCl, pH 7.2-7.4, 150 mM NaCl, and 0.1% Tween-20), they were incubated against the secondary antibody 1:2000 IRDye 800CW goat anti-rabbit IgG (Cat. #926-32211; LI-COR Biosciences, Lincoln, NE, USA), or 1:2000 IRDye 800CW goat anti-mouse IgG (Cat. #926-32211; LI-COR Biosciences) for 2 hours at room temperature. The membranes were washed again three times in TBST, followed by visualization of protein bands using the Odyssey Infrared Imaging System (LI-COR Biosciences). Densitometric analysis of protein bands was performed using ImageJ software (version 1.48v; National Institutes of Health [NIH], Bethesda, MD, USA; https://imagej.nih.gov/ij). Values were normalized to those of the β-actin or α-tubulin loading control. All Western blots shown are representative of at least three independent experiments.

Statistical Analysis

All data were analyzed using GraphPad Prism software (version 8.3.0; GraphPad Inc., San Diego, CA, USA). The Shapiro-Wilk normality test was used to analyze the distribution of all data sets. Multiple comparisons were performed using 1-way ANOVA with Bonferroni's post hoc tests (for normally distributed data), Kruskal-Wallis non-parametric test with Dunn's post hoc test (for non-normally distributed data), or 2-way ANOVA with Bonferroni's post hoc tests or original false discovery rate (FDR) method of Benjamini and Hochberg. A 2-way repeated-measure ANOVA (RM-ANOVA) was used to assess the effect of scleral *Hif-2α* knockdown on normal refractive development in mice at different times. The P values < 0.05 were considered statistically significant.

Results

FD Induces Increases in Scleral HIF-2α Expression

To determine if there is an association between scleral HIF-2α expression and myopia development, we performed FDM induction in wild type C57BL/6J mice for either 2 days, or

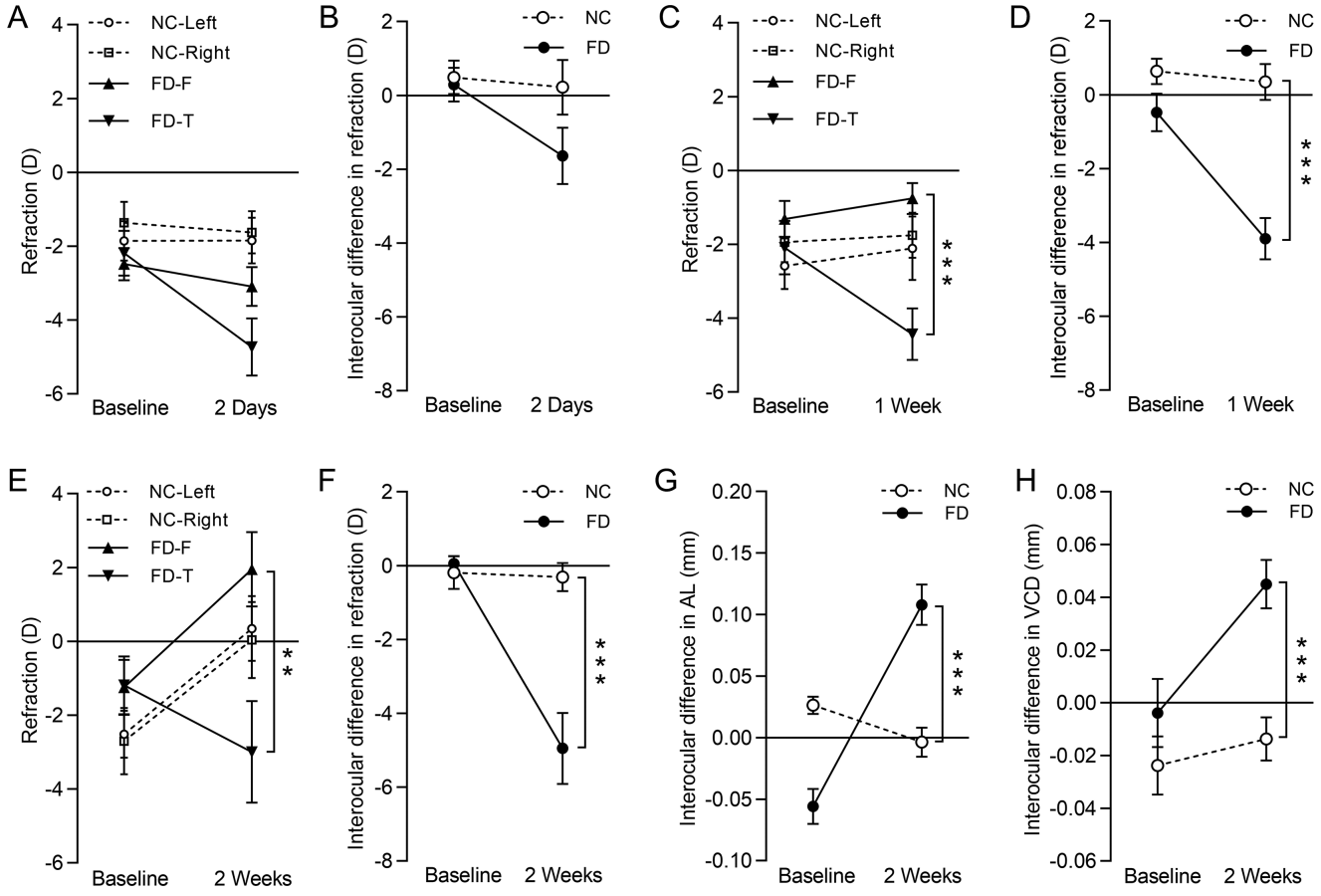

Figure 1. Refraction, AL, and VCD changes after 2 days, 1 week, or 2 weeks of FDM induction in wild type C57BL/6J mice. (**A**) Refraction after 2 days of FD; (**B**) Interocular differences (value for FD-T/right eyes minus that for FD-F/left eyes) in refraction after 2 days of FD; (**C**) Refraction after 1 week of FD; (**D**) Interocular difference in refraction after 1 week of FD; (**E**) Refraction after 2 weeks of FD; (**F–H**) Interocular differences in refraction (**F**), AL (**G**), and VCD (**H**) after 2 weeks of FD. n = 8, 8, and 8 NC mice for 2 days, 1 week, or 2 weeks groups, n = 8, 8, and 8 FD mice for 2 days, 1 week, or 2 weeks groups. Data are expressed as mean ± SEM. $^{**}P < 0.01$; $^{***}P < 0.001$; 2-way RM-ANOVA with Bonferroni's post hoc. Baseline, before FD; 2 weeks, 2 weeks after FD. D, diopter.

Investigative Ophthalmology & Visual Science

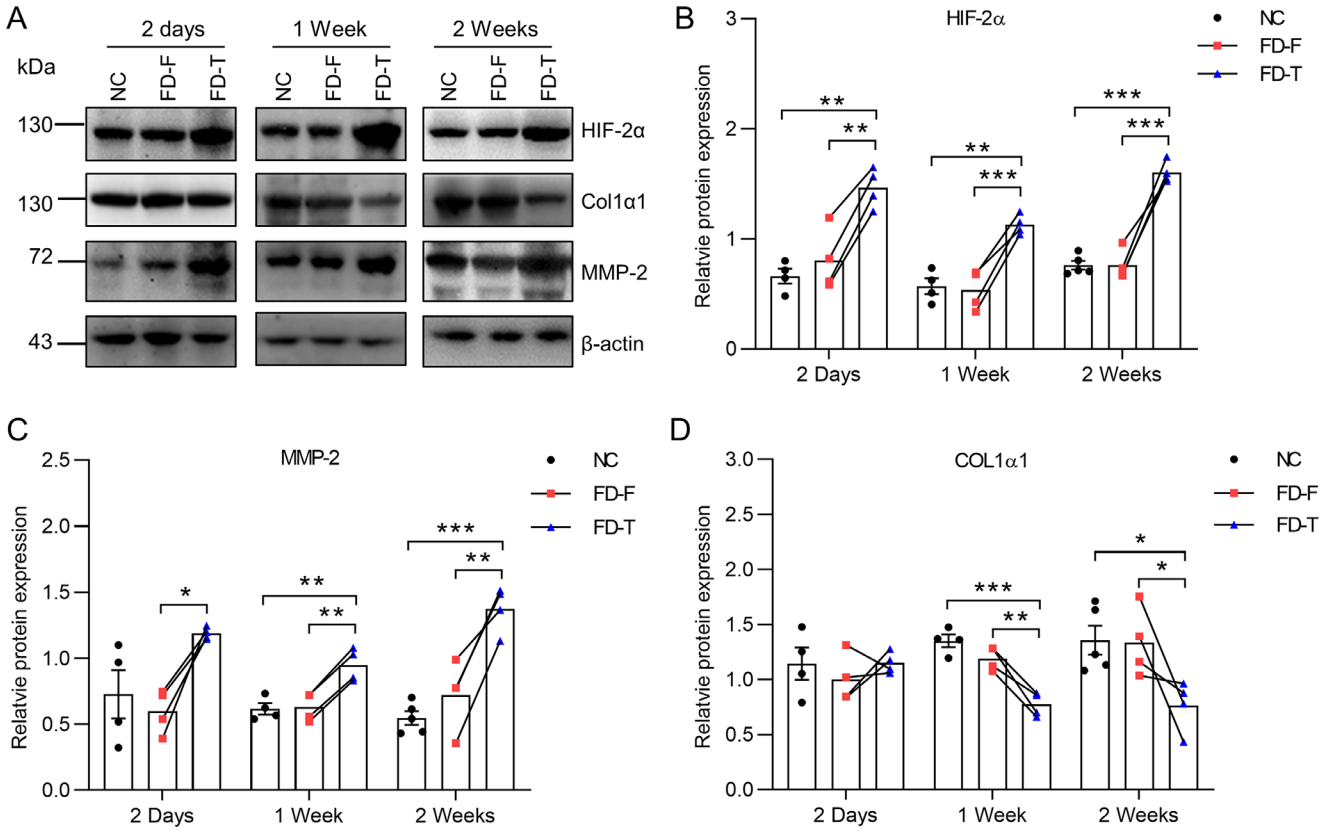

Figure 2. FD induces rises in scleral HIF-2α expression. (**A**) Levels of scleral HIF-2α, MMP-2, and COL1α1 proteins, determined by western blot analysis after 2 days, 1 week, or 2 weeks of FD induction; β-actin was the loading control. (**B–D**) Densitometric quantification of western blot results of HIF-2α (**B**), MMP-2 (**C**), and COL1α1 (**D**). Each data point represents an independent mouse; $n = 4$, 4 and 5 NC mice for 2 days, 1 week, or 2 weeks groups, $n = 4$, 4, and 4 FD mice for 2 days, 1 week, or 2 weeks groups. Data are expressed as means ± SEM. *$P < 0.05$, **$P < 0.01$; ***$P < 0.001$; 1-way ANOVA with Bonferroni's post hoc tests. FD-T: Right eye of each mouse in FD groups were subjected to FD; FD-F: Left eyes of each mouse in FD groups; NC: age-matched mice without FD induction. D, diopter.

1 or 2 weeks and then determined the scleral HIF-2α expression levels at each time point.

After 2 days of FD, no significant myopia was induced (Figs. 1A, 1B; Fig. 1A, $F_{(3, 28)} = 3.602$, $P = 0.0256$, FD-F versus FD-T: $P = 0.3158$; Fig. 1B, $F_{(1, 14)} = 2.403$, $P = 0.1434$, FD versus NC: $P = 0.0870$). Nevertheless, the scleral HIF-2α protein levels in the FD-T eyes were already significantly higher than those in the FD-F and NC groups (Figs. 2A, 2B; $F_{(2, 9)} = 17.19$, $P = 0.0008$; FD-T versus NC: $P = 0.0012$; FD-T versus FD-F: $P = 0.0043$). Consistent with our previous results,[9] the scleral MMP-2 expression levels in the FD-T group were higher than those in the FD-F eyes (see Figs. 2A, 2C; $F_{(2, 9)} = 6.994$, $P = 0.0147$; FD-T versus FD-F: $P = 0.0185$). However, there were no significant differences in scleral COL1α1 expression levels among the FD-T, FD-F, and NC groups (see Figs. 2A, 2D; $F_{(2, 9)} = 0.5769$, $P = 0.5797$).

In the FD-T eyes, 1 week of FD led to a significant myopic shift in refraction (Figs. 1C, 1D; Fig. 1C, $F_{(3, 28)} = 2.721$, $P = 0.0633$, FD-F versus FD-T: $P = 0.0008$; Fig. 1D, $F_{(1, 14)} = 25.14$, $P = 0.0002$, FD-F versus FD-T: $P < 0.0001$). This myopic shift was accompanied by higher HIF-2α (see Figs. 2A, 2B; $F_{(2, 9)} = 21.79$, $P = 0.0004$; FD-T versus NC: $P = 0.0011$; FD-T versus FD-F: $P = 0.0007$) and MMP-2 (see Figs. 2A, 2C; $F_{(2, 9)} = 12.30$, $P = 0.0027$; FD-T versus NC: $P = 0.0052$; FD-T versus FD-F: $P = 0.0070$) expression levels and lower COL1α1 accumulation (see Figs. 2A, 2D; $F_{(2, 9)} = 28.83$, $P = 0.0001$; FD-T versus NC: $P = 0.0001$; FD-T versus FD-F: $P = 0.0015$) in the FD-T eyes as compared with FD-F and NC groups.

After 2 weeks of FD, the FD-T eyes continued to exhibit significant myopic shift in refraction (see Figs. 1E, 1F; Fig. 1E, $F_{(3, 28)} = 1.400$, $P = 0.2634$, FD-F versus FD-T: $P = 0.0028$; Fig. 1F, $F_{(1, 14)} = 11.50$, $P = 0.0044$, FD-F versus FD-T: $P < 0.0001$) and elongation of AL (see Fig. 1G; $F_{(1, 14)} = 0.7992$, $P = 0.3865$, FD-F versus FD-T: $P < 0.0001$) and VCD (see Fig. 1H; $F_{(1, 14)} = 12.47$, $P = 0.3865$, FD-F versus FD-T: $P = 0.0033$). Expression pattern changes of scleral HIF-2α (see Figs. 2A, 2B; $F_{(2, 10)} = 83.46$, $P < 0.0001$; FD-T versus NC: $P < 0.0001$; FD-T versus FD-F: $P < 0.0001$), MMP-2 (see Figs. 2A, 2C; $F_{(2, 10)} = 22.97$, $P = 0.0002$; FD-T versus NC: $P = 0.0002$; FD-T versus FD-F: $P = 0.0018$), and COL1α1 (see Figs. 2A, 2D; $F_{(2, 10)} = 5.866$, $P = 0.0206$; FD-T versus NC: $P = 0.0110$; FD-T versus FD-F: $P = 0.0171$) expression levels in the NC, FD-F, and FD-T eyes were similar with those measured after 1 week of FD.

Taken together, there is a correspondence between increases in HIF-2α and MMP-2 expression levels, and declines in COL1α1 accumulation during myopia development.

Investigative Ophthalmology & Visual Science

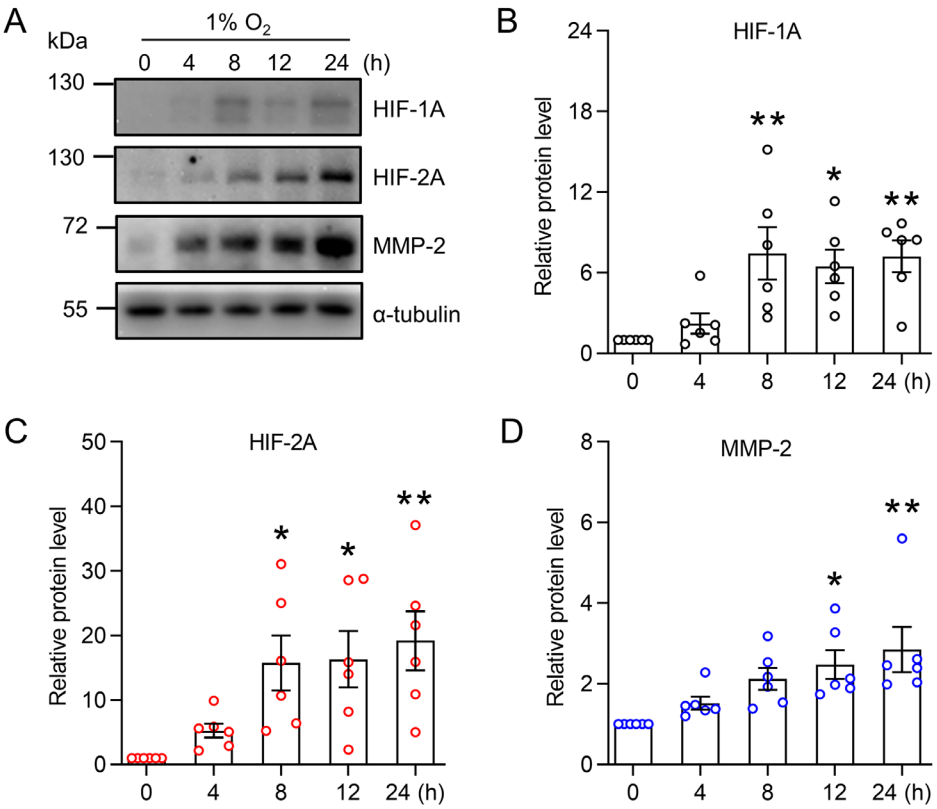

Figure 3. Hypoxia increases MMP-2 expression in HSFs. (**A**) Western blot analysis of HIF-1A, HIF-2A, and MMP-2 protein levels in HSFs exposed to 1% O_2. α-tubulin was used as loading control. (**B–D**) Densitometric quantification of Western blot results of HIF-1A (**B**), HIF-2A (**C**), and MMP-2 (**D**), respectively ($n = 6$). Data are expressed as mean ± SEM. *$P < 0.05$; **$P < 0.01$; 1-way ANOVA with Bonferroni's post hoc tests.

Selective HIF-2A Silencing Antagonizes Hypoxia-Induced MMP-2 Upregulation in HSFs

To determine if hypoxia stimulates the MMP-2 expression levels in HSFs, we incubated HSFs under a hypoxic condition (i.e. 1% oxygen) for 4, 8, 12, or 24 hours. The cells incubated under a normoxic condition (i.e. 21% oxygen) served as the control. Consistent with our previous results, exposing HSFs to 1% oxygen upregulated the protein expression of HIF-1A (Figs. 3A, 3B; $F_{(4, 25)} = 6.261$, $P = 0.0012$). In addition, hypoxic treatment enhanced HIF-2A (see Figs. 3A, 3C; $F_{(4, 25)} = 5.214$, $P = 0.0034$) and MMP-2 expression levels (see Figs. 3A, 3D; $F_{(4, 25)} = 5.085$, $P = 0.0039$).

To explore if HIF-1A or/and HIF-2A mediates this hypoxia-induced MMP-2 upregulation, we transfected HSFs with siRNA that selectively targeted each of these two genes. HIF-1A (Figs. 4A–C; main effect of HIF-1A knockdown: HIF-1A, $F_{(3, 24)} = 5.799$, $P = 0.0040$; HIF-2A, $F_{(3, 24)} = 0.5325$, $P = 0.6644$) or HIF2A (Figs. 5A–C; main effect of HIF-2A knockdown: HIF-2A, $F_{(3, 24)} = 5.032$, $P = 0.0076$; HIF-1A, $F_{(3, 24)} = 0.0525$, $P = 0.9838$) expression levels were selectively reduced post-transfection. HIF-1A knockdown had no significant effect on hypoxia-induced upregulation of MMP-2 (see Figs. 4A, 4D; main effect of HIF-1A knockdown: $F_{(3, 24)} = 2.208$, $P = 0.1133$). However, HIF-2A knockdown significantly suppressed such MMP-2 increases (Figs. 5A, 5D; main effect of HIF-2A knockdown: $F_{(3, 24)} = 8.607$, $P = 0.0005$). In addition, neither HIF-1A nor HIF-2A knockdown had significant effects on MMP-2 expression under the normoxic condition (i.e. 21% oxygen; see Figs. 4A, 4D, 5A, 5D).

Taken together, these in vitro studies implicate a potential role for HIF-2A, rather than HIF-1A, in mediating the hypoxia-induced MMP-2 upregulation.

Scleral HIF-2α Knockdown Induces Hyperopia and Suppresses FDM Development

To assess if HIF-2α mediates scleral MMP-2 upregulation during myopia development, we established a scleral HIF-2α knockdown mouse model. This was achieved by sub-Tenon's capsule injection of AAV8-Cre virus in *HIF-2α*$^{fl/fl}$ mice. *HIF-2α*$^{fl/fl}$ mice injected with AAV8-vector served as the control.

In the first stage, we determined if scleral HIF-2α knockdown altered the normal refraction development without FDM induction. At 4 weeks after AAV8-Cre injection, scleral HIF-2α mRNA levels were significantly lower than those in the AAV8-vector injected eyes (Fig. 6A; $F_{(3, 24)} = 4.115$, $P = 0.0173$; AAV8-Cre versus AAV8-vector injected eyes: $P = 0.0379$). This procedure selectively reduced *Hif-2α* gene expression only in the sclera, while it had no significant effect on *Hif-2α* mRNA expression levels in the retina (see Fig. 6B; $F_{(3, 24)} = 0.5174$, $P = 0.6743$; AAV8-Cre versus AAV8-vector injected eyes: $P = 0.3621$), and cornea (see Fig. 6C; $F_{(3, 24)} = 0.8248$, $P = 0.4931$; AAV8-Cre versus AAV8-vector injected eyes: $P = 0.2244$) in AAV8-Cre injected

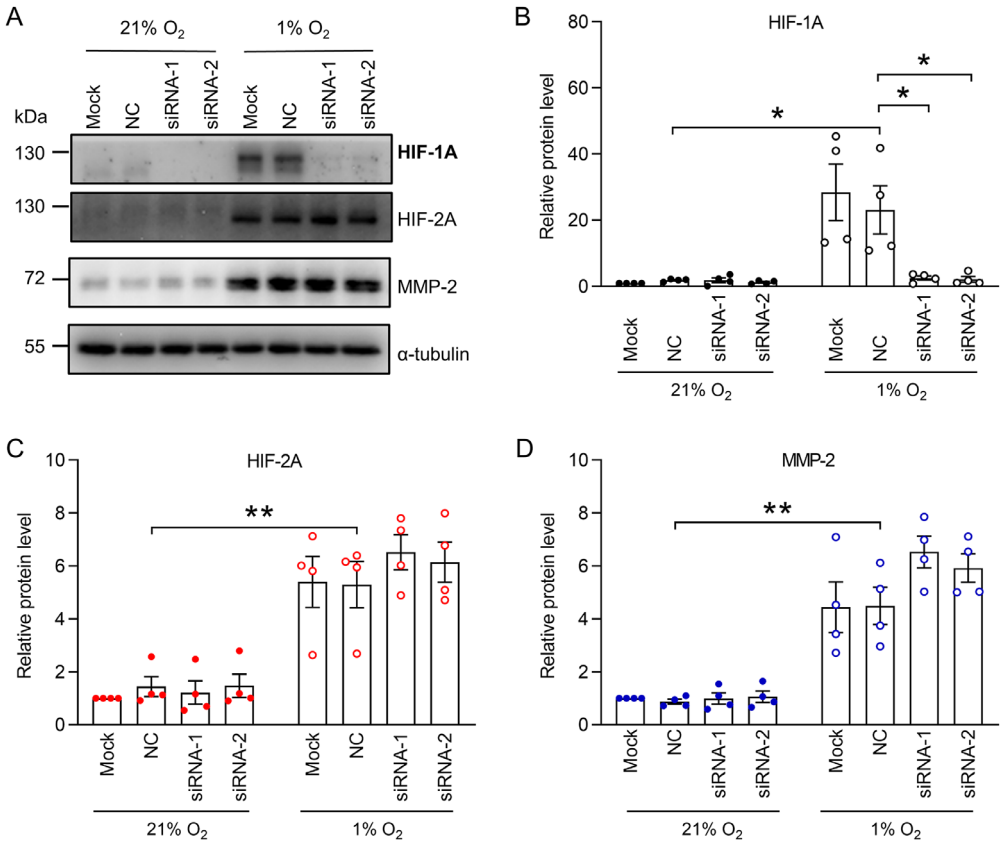

Figure 4. HIF-1A knockdown does not suppress hypoxia-induced MMP-2 upregulation in HSFs. HSFs transfected with siRNA targeting *Hif-1α* were exposed to 1% O_2 for 24 hours. (**A**) Western blot analysis of HIF-1A, HIF-2A, and MMP-2 protein levels in HSFs exposed to 1% O_2. The α-tubulin was used as the loading control. (**B-D**) Densitometric quantification of western blot results of HIF-1A (**B**), HIF-2A (**C**), and MMP-2 (**D**), respectively ($n = 4$). Data in **B** to **D** represent the means ± SEM. Mock: blank control (transfection reagent only); NC, normal control (cells transfected with scrambled normal control siRNA). *$P < 0.05$; **$P < 0.01$; 2-way ANOVA with Bonferroni's post hoc tests.

eyes as compared with those in AAV8-vector injected eyes. Consistent with the mRNA expression levels, scleral HIF-2α protein levels were also lower in the AAV8-Cre injected eyes compared to the AAV8-vector injected eyes (Figs. 7A, 7B; $F_{(3, 12)} = 9.090$, $P = 0.0021$; AAV8-Cre versus AAV8-vector injected eyes: $P = 0.0162$). In addition, this procedure had no significant effect on scleral HIF-1α protein levels (see Figs. 7A, 7C; $F_{(3, 12)} = 0.7974$, $P = 0.5187$; AAV8-Cre versus AAV8-vector injected eyes: $P > 0.9999$). Levels of scleral MMP-2 (see Figs. 7A, 7D; $F_{(3, 20)} = 0.0517$, $P = 0.9837$; AAV8-Cre versus AAV8-vector injected eyes: $P > 0.9999$) and COL1α1 (see Figs. 7A, 7E; $F_{(3, 20)} = 1.042$, $P = 0.4094$; AAV8-Cre versus AAV8-vector injected eyes: $P = 0.7216$) were also not significantly different between AAV8-Cre and AAV8-vector groups.

Even though the refractive development rose in both the AAV8-Cre and AAV8-vector injected eyes, the refraction of the AAV8-Cre injected eyes was relatively more hyperopic than the AAV8-vector injected eyes (Figs. 8A, 8B; Fig. 8A: effect of HIF-2α knockdown: $F_{(3, 34)} = 4.107$, $P = 0.0137$, AAV8-Cre injected eyes versus AAV8-vector injected eyes after 4 weeks of injection, $P = 0.0279$; Fig. 8B: effect of HIF-2α knockdown: $F_{(1, 17)} = 0.09690$, $P = 0.7594$). The AL elongation (Fig. 8C; effect of HIF-2α knockdown: $F_{(1, 17)} = 0.1310$, $P = 0.7218$) and VCD increases (Fig. 8D; effect of HIF-2α knockdown: $F_{(1, 17)} = 0.2332$, $P = 0.6354$) were also not significantly different between the AAV8-Cre eyes and the AAV8-vector eyes. Because the baseline data of AAV8-vector and AAV8-Cre groups were already different from one another, we also showed the changes from baseline data to after 2 and 4 weeks of AAV8 injection (Figs. 8E–G). The refraction (see Fig. 8E; $F_{(3, 34)} = 1.340$, $P = 0.2778$), AL (see Fig. 8F; $F_{(3, 34)} = 0.2516$, $P = 0.8597$), and VCD (Fig. 8G; $F_{(3, 34)} = 1.973$, $P = 0.1365$) changes between AAV8-vector and AAV8-Cre groups were not significantly different at the given time points.

In the second stage of this analysis, we determined if scleral HIF-2α knockdown altered FDM development. After 2 weeks of FD, the protein levels of HIF-2α (Figs. 9A, 9B; effect of FD: $F_{(1, 20)} = 9.695$, $P = 0.0055$; FD-F versus FD-T eyes: $P = 0.0032$), HIF-1α (see Figs. 9A, 9C; effect of FD: $F_{(1, 20)} = 35.99$, $P < 0.001$; FD-F versus FD-T eyes: $P = 0.0007$), and MMP-2 (see Figs. 9A, 9D; effect of FD: $F_{(1, 20)} = 10.38$, $P = 0.0043$; FD-F versus FD-T eyes: $P = 0.0117$) in the sclera were significantly higher in FD-T eyes than those in FD-F eyes in the AAV8-vector group. The COL1α1 protein level was lower in FD-T eyes than that in FD-F eyes in the AAV8-vector group (see Figs. 9A, 9E; effect of FD: $F_{(1, 20)} = 5.513$, $P = 0.0293$; FD-F versus FD-T eyes: $P = 0.0159$). However, the higher HIF-2α (see Figs. 9A, 9B; $P > 0.9999$) and MMP-2 (see Figs. 9A, 9D; $P > 0.9999$) expression, along with lower COL1α1 accumulation (see Figs. 9A, 9E; $P > 0.9999$) was not observed between FD-F and FD-T eyes in AAV8-Cre mice. The scleral HIF-2α levels were lower in FD-T eyes of

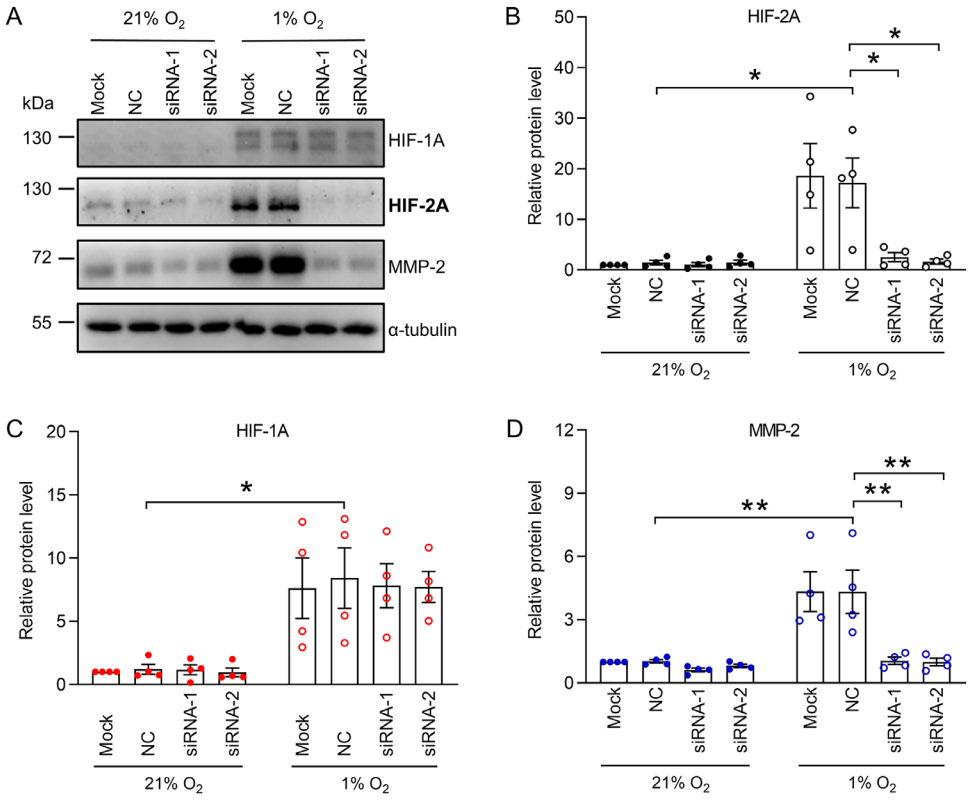

Figure 5. HIF-2A knockdown blocks hypoxia-induced MMP-2 upregulation in HSFs. HSFs transfected with siRNA targeting *Hif-2α* were exposed to 1% O_2 for 24 hours. (**A**) Western blot analysis of HIF-2A, HIF-1A, and MMP-2 protein levels in HSFs exposed to 1% O_2. The α-tubulin was used as loading control. (**B-D**) Densitometric quantification of western blot results of HIF-2A (**B**), HIF-1A (**C**), and MMP-2 (**D**), respectively ($n = 4$). Data in **B** to **D** represent the means ± SEM. Mock: blank control (transfection reagent only); NC, normal control (cells transfected with scrambled normal control siRNA). *$P < 0.05$; **$P < 0.01$; 2-way ANOVA with Bonferroni's post hoc tests.

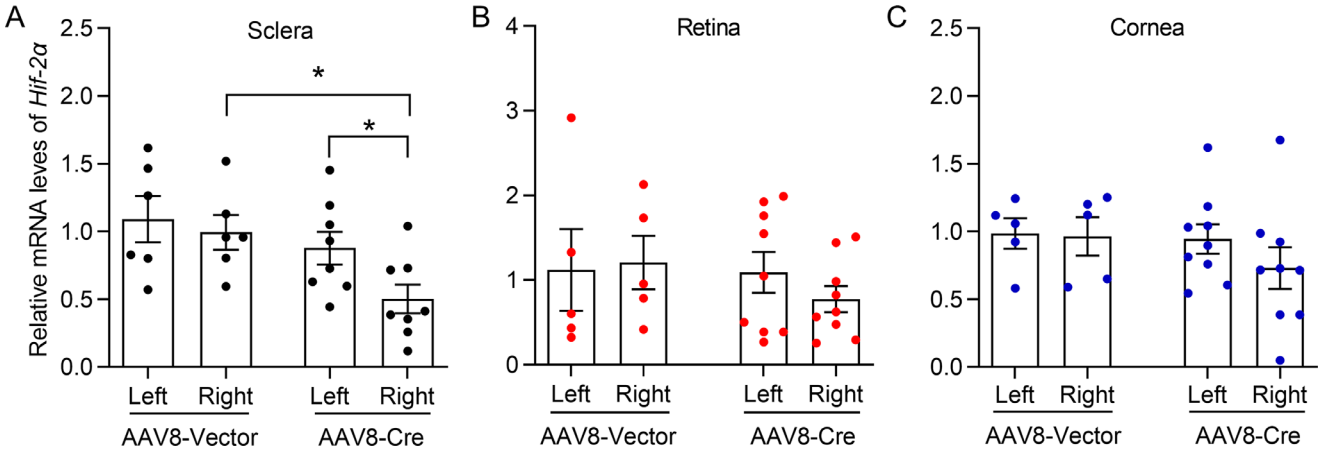

Figure 6. The qRT-PCR analysis of Hif-2α mRNA expression levels in the sclera, retina, and cornea. (**A-C**) The qRT-PCR analysis of scleral *Hif-2α* mRNA expression in sclera (**A**), retina (**B**), and cornea (**C**). Expression levels were normalized to those of the "Left" of the "AAV8-vector" control, and *18s rRNA* was used as the reference gene. Each data point represents an independent mouse. $n = 6$, 5, and 5 AAV8-vector mice for sclera, retina, and cornea; $n = 8$, 9, and 9 AAV8-Cre mice for sclera, retina, and cornea. Data are expressed as means ± SEM. *$P < 0.05$; 1-way ANOVA, original FDR method of Benjamini and Hochberg was used. Right: The right eye of each *Hif-2α*$^{fl/fl}$ mouse was injected with AAV8-Cre or AAV8-vector control; Left: the left eyes served as the fellow non-injected control.

AAV8-Cre group, compared with the FD-T eyes of AAV8-vector group (see Figs. 9A, 9B; main effect of HIF-2α knockdown: $F_{(1, 20)} = 2.218$, $P = 0.1520$; FD-T eyes of AAV8-Cre group versus AAV8-vector group: $P = 0.0401$). Moreover, scleral HIF-2α knockdown had no significant effect on FD-induced HIF-1α upregulation (see Figs. 9A, 9C; main effect of HIF-2α knockdown: $F_{(1, 20)} = 0.03656$, $P = 0.8503$; FD-T eyes of AAV8-Cre group versus AAV8-vector group: $P > 0.9999$). In addition, the COL1α1 expression was higher in FD-T eyes in AAV8-Cre mice, compared with the FD-T eyes of AAV8-vector mice (see Figs. 9A, 9E; main effect of HIF-2α knockdown: $F_{(1, 20)} = 8.340$, $P = 0.0091$;

Investigative Ophthalmology & Visual Science

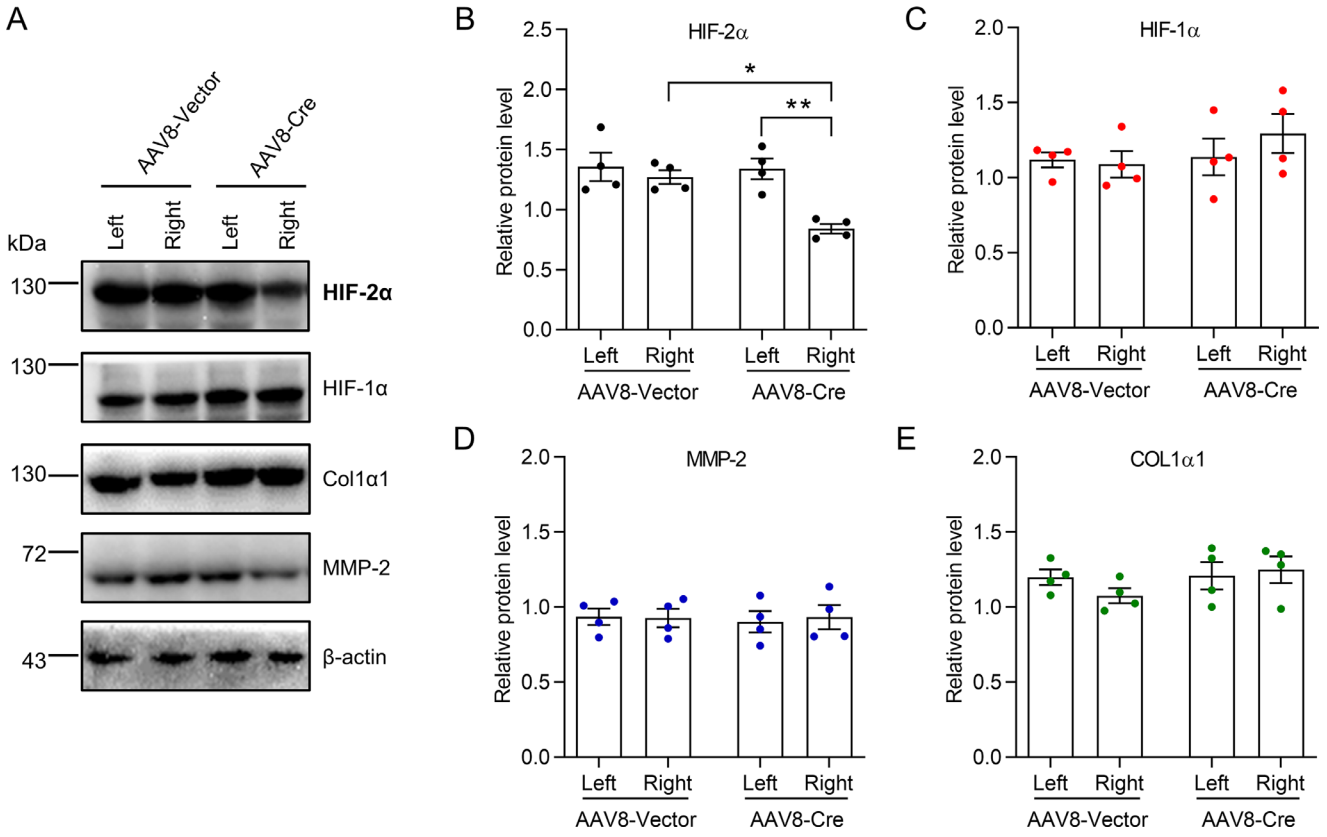

Figure 7. Western blot analysis of HIF-2α and MMP-2 expression levels in AAV8 injected *Hif-2α$^{fl/fl}$* mice. (**A**) Protein levels of scleral HIF-2α, HIF-1α, MMP-2, and COL1α1 expression 4 weeks after AAV8 injection; β-actin was used as the loading control. (**B-E**) Densitometric quantification of Western blot results of HIF-2α (**B**), HIF-1α (**C**), MMP-2 (**D**), and COL1α1 (**E**), respectively ($n = 4$). Each data point represents an independent mouse. Data in **B** to **E** represent the means ± SEM. *$P < 0.05$; **$P < 0.01$; 1-way ANOVA with Bonferroni's post hoc tests.

FD-T eyes of AAV8-Cre group versus AAV8-vector group: $P = 0.0065$).

After 2 weeks of FD, significant myopia was induced in the FD-T eyes compared to the respective FD-F eyes in the AAV8-vector group, but not in the AAV8-Cre group (Fig. 10A; effect of FD: $F_{(3, 36)} = 2.782$, $P = 0.0549$; AAV8-vector FD-F versus FD-T eyes: $P = 0.0317$; AAV8-Cre FD-F versus FD-T eyes: $P = 0.1982$). This suppression of myopia development in the AAV8-Cre group was in parallel with the reduction in scleral HIF-2α protein level (Fig. 10B; main effect of HIF-2α knockdown: $F_{(1, 18)} = 6.913$, $P = 0.0170$). However, the increases in AL (Fig. 10C; main effect of HIF-2α knockdown: $F_{(1, 18)} = 0.482$, $P = 0.0411$; 2 weeks AAV8-vector versus AAV8-Cre: $P = 0.1991$) and VCD (Fig. 10D; main effect of HIF-2α knockdown: $F_{(1, 18)} = 0.8112$, $P = 0.3797$; 2 weeks AAV8-vector versus AAV8-Cre: $P = 0.7440$) in AAV8-Cre mice and in AAV8-vector mice were not statistically significant.

Taken together, these data indicate that the knockdown of scleral HIF-2α had no significant effect on normal refraction development, but it inhibited FD-induced scleral MMP-2 upregulation and myopia development.

Scleral HIF-1α Knockdown Suppresses Myopia Development Without Mediating MMP-2 Upregulation

In our previous study, we showed that scleral HIF-1α knockdown suppressed FD-induced declines in COL1α1 accumulation and myopia development.[14] To investigate whether scleral HIF-1α contributes to COL1α1 degradation during myopia development, we established a scleral HIF-1α knockdown mouse model. This was achieved by sub-Tenon's capsule injection of AAV8-Cre virus in *HIF-1α$^{fl/fl}$* mice, as previously described.[12] *HIF-1α$^{fl/fl}$* mice injected with AAV8-vector served as the control.

After 2 weeks of FD, the protein levels of scleral HIF-1α (Figs. 11A, 11B; effect of FD: $F_{(1, 20)} = 12.99$, $P < 0.001$; FD-F versus FD-T eyes: $P < 0.001$), HIF-2α (see Figs. 11A, 11C; effect of FD: $F_{(1, 20)} = 68.65$, $P < 0.001$; FD-F versus FD-T eyes: $P = 0.0002$), and MMP-2 (see Figs. 11A, 11D; effect of FD: $F_{(1, 20)} = 21.06$, $P = 0.0002$; FD-F versus FD-T eyes: $P = 0.0228$) were significantly higher in FD-T eyes than those in FD-F eyes in the AAV8-vector group. The COL1α1 protein level was lower in FD-T eyes than that in FD-F eyes in the AAV8-vector group (see Figs. 11A, 11E; effect of FD: $F_{(1, 20)} = 12.78$, $P = 0.0019$; FD-F versus FD-T eyes: $P = 0.0026$). These higher HIF-2α (see Figs. 11A, 11C; $P < 0.001$) and MMP-2 (see Figs. 11A, 11D; $P = 0.026$) expression levels were also observed in the FD-T eyes than in those in the FD-F eyes in AAV8-Cre mice. However, the higher HIF-1α expression levels (see Figs. 11A, 11B; $P > 0.9999$) along with lower COL1α1 accumulation (see Figs. 11A, 11E; $P > 0.9999$) were not observed between the FD-F and FD-T eyes in AAV8-Cre mice. Moreover, scleral HIF-1α knockdown had no significant effect on FD-induced upregulation of MMP-2 (see Figs. 11A, 11D; main effect of HIF-1α knockdown: $F_{(1, 20)} = 0.7899$, $P = 0.3847$; FD-T eyes of AAV8-Cre

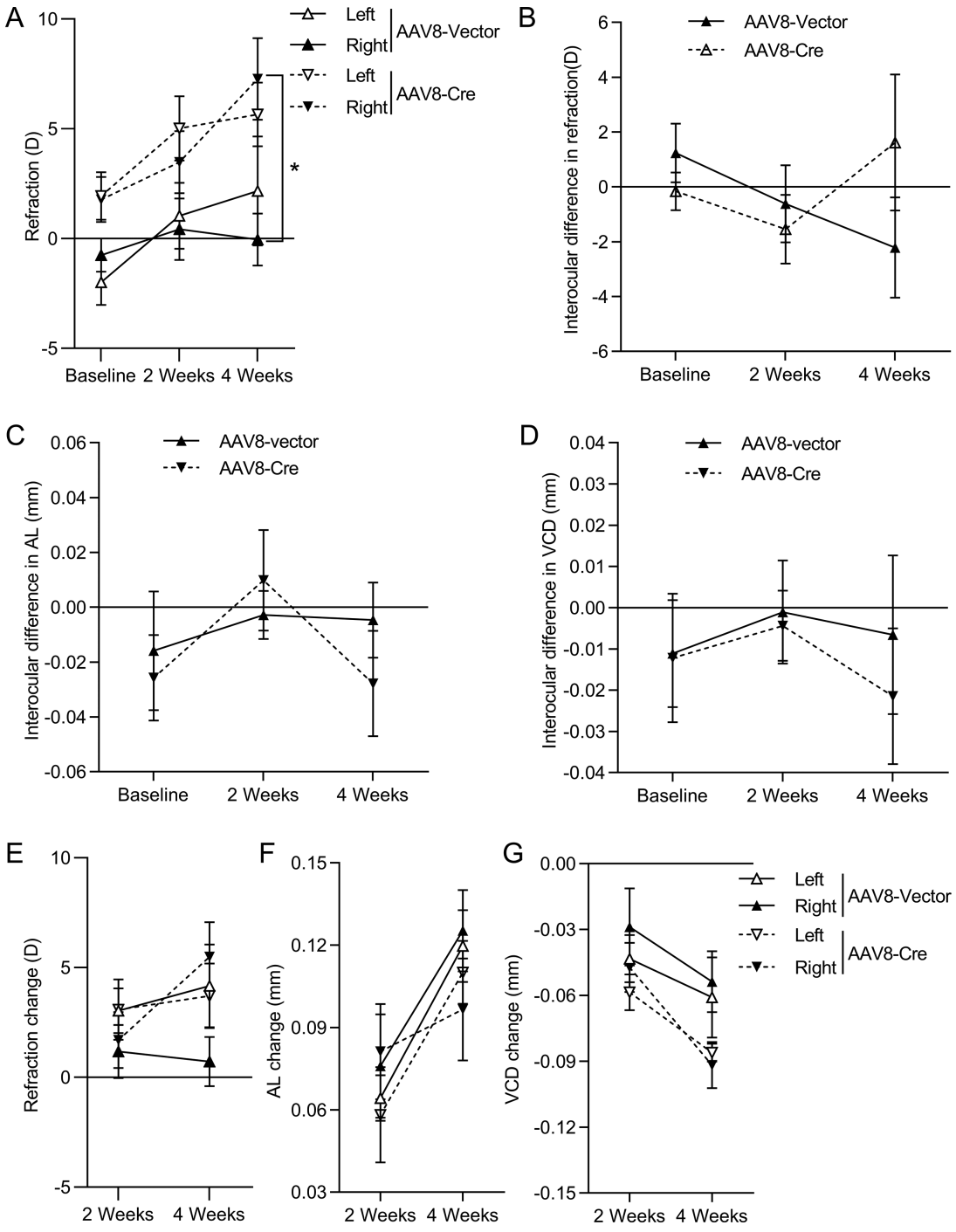

Figure 8 Effect of scleral HIF-2α knockdown on ocular parameters 2 and 4 weeks after injection. (**A**) Refraction of non-injected left eyes and AAV8 injected right eyes in the two groups before and 2 weeks and 4 weeks after AAV8 injection. (**B-D**) Inter-ocular differences in refraction (**B**), AL (**C**), and VCD (**D**). (**E-G**) Refraction (**E**), AL (**F**), and VCD (**G**) changes from baseline after 2 and 4 week of AAV8-vector and AAV8-Cre injection (values of 2 or 4 weeks minus baseline values). Data are expressed as means ± SEM. *$P < 0.05$; 2-way RM-ANOVA with Bonferroni's post hoc tests; $n = 9$ and 10 for AAV8-vector and AAV8-Cre mice, respectively. D, diopter.

group vesus AAV8-vector group: $P > 0.9999$) and HIF-2α (see Figs. 11A, 11C; main effect of HIF-1α knockdown: $F_{(1, 20)} = 0.7567$, $P = 0.3944$; FD-T eyes of AAV8-Cre group versus AAV8-vector group: $P > 0.9999$).

Taken together, these data indicate that the knockdown of scleral HIF-1α inhibited FD-induced declines in collagen accumalation and myopia development without affecting scleral MMP-2 upregulation.

Discussion

In the current study, we first found that scleral HIF-2α underwent upregulation accompanied myopia development in mice. This response is similar to that by HIF-1α, which we described in our previous study.[11] This similarity indicated that both the HIF-1α and HIF-2α were involved in myopia development. Moreover, in vitro results from the

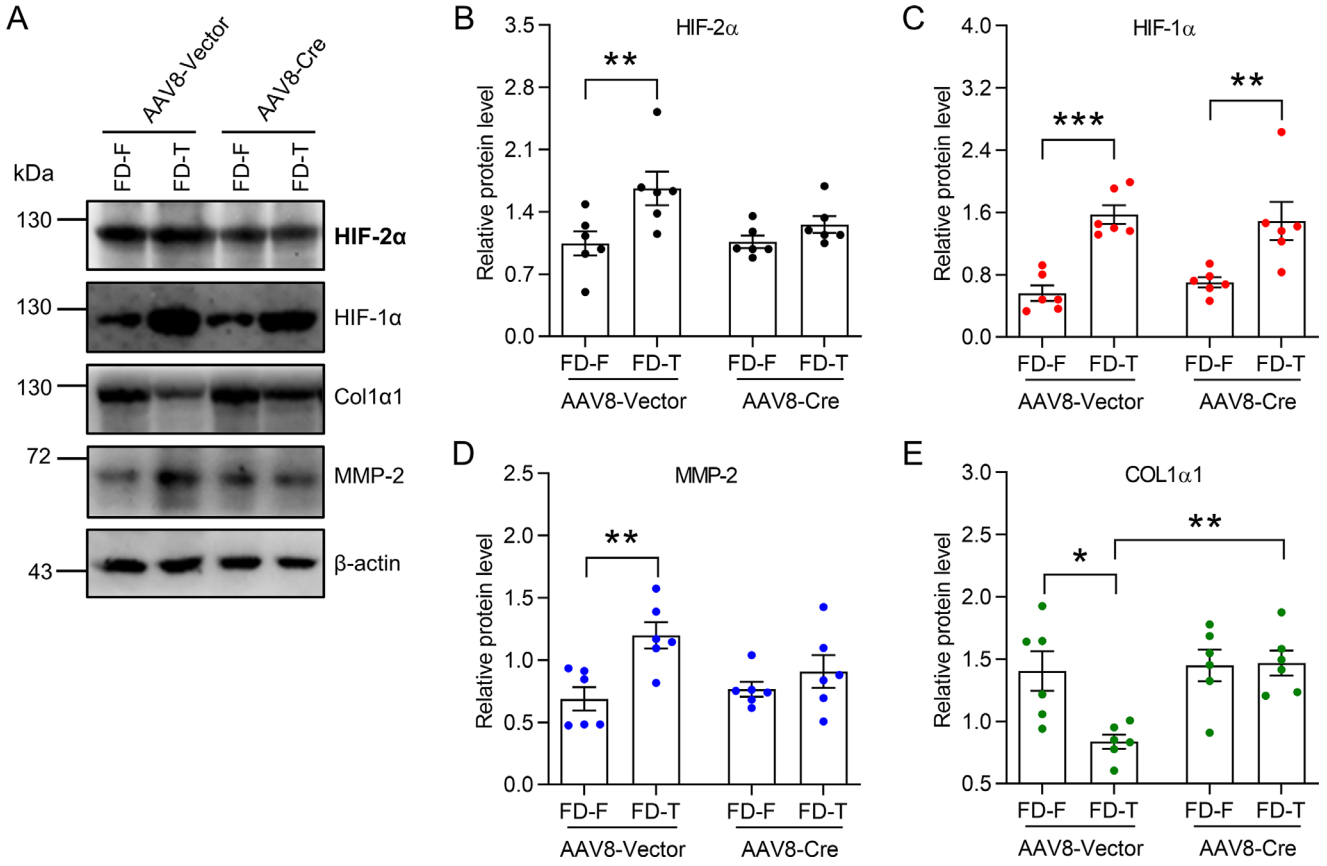

Figure 9. Western blot analyses of FD-treated scleral HIF-2α knockdown mice. Sub-Tenon's space in the right eye of *Hif-2α*$^{fl/fl}$ mice were injected with AAV8-vector or AAV8-Cre. After 1 week, myopia was induced for 2 additional weeks in the right eye (FD-T), while the left eye served as non-FD fellow-eye control (FD-F). (**A**) Protein levels of scleral HIF-2α, HIF-1α, MMP-2, and COL1α1 after 2 week of myopia induction; β-actin was used as the loading control. (**B-D**) Densitometric quantification of Western blot results of HIF-2α (**B**), HIF-1α (**C**), MMP-2 (**D**), and COL1α1 (**E**), respectively ($n = 6$). Each data point represents an independent mouse. Data in **B** to **E** represent the means ± SEM. *$P < 0.05$; **$P < 0.01$; ***$P < 0.001$; 2-way ANOVA with Bonferroni's post hoc tests.

current study showed that hypoxia induced MMP-2 upregulation was dependent on HIF-2A rather than HIF-1A expression. Furthermore, the in vivo studies showed that knocking down HIF-2α in the sclera significantly suppressed the FD-induced myopia development. This inhibition accompanied suppression of both FD-induced upregulation of MMP-2 and declines in COL1α1 content in the sclera. However, the FD-indued upregulation of MMP-2 was not altered in scleral HIF-1α knockdown mice. Collectively, these findings demonstrate that scleral hypoxia upregulates HIF-2α and promotes myopia development through enhancing MMP-2 expression and collagen degradation. This study not only clarifies the mechanism underlying scleral collagen degradation but also confirms the role of hypoxia in inducing scleral ECM remodeling during myopia development.

It is generally accepted that eye growth is regulated by different homeostatic control mechanisms.[6] The visual input triggers a cascade of retinal signaling processes that ultimately induces biochemical responses leading to scleral ECM remodeling. Excessive or insufficient ocular growth causes the image to be focused either in the front (myopia) or behind (hyperopia) the retinal photoreceptors. We have shown that FD upregulated both the HIF-1α[12] and HIF-2α (the current study) expression in the sclera and promoted myopia development. In addition, either HIF-1α[12] or HIF-2α (the current study) knockdown in the sclera induced hyperopia under a normal visual environment without myopia induction.[12] These findings highlight the importance of the HIFs as growth regulators in scleral homeostasis. Sustaining the HIFs contents at a physiological level might be critical for normal refractive development.

The steady state level of collagen accumulation is dependent on the balance between its net rates of synthesis and degradation. Declines in scleral collagen accumulation are a consequence of both reduced synthesis and increased degradation.[8] This study indicated an involvement of hypoxia in regulating the collagen degradation process, however, whether hypoxia contributes to suppressed collagen synthesis is yet to be determined. Several different studies reported the involvement of hypoxia in controlling collagen synthesis, modification and organization in other tissues.[27–29] In addition, hypoxia was also reported to inhibit COL1A1 gene expression in a HIF-1α dependent way in human fibroblasts.[30,31] Further studies are warranted to clarify the role of hypoxia in modulating collagen synthesis in the sclera.

This study demonstrates that HIF-2α contributes to mediating hypoxia induced MMP-2 upregulation that induces declines in collagen accumulation and increases in myopia progression in an experimental mouse model. Using this same model, we defined similar roles for scleral fibroblasts[9] and macrophages[10] in mediating MMP-2 upregulation during myopia development. In the current study,

Investigative Ophthalmology & Visual Science

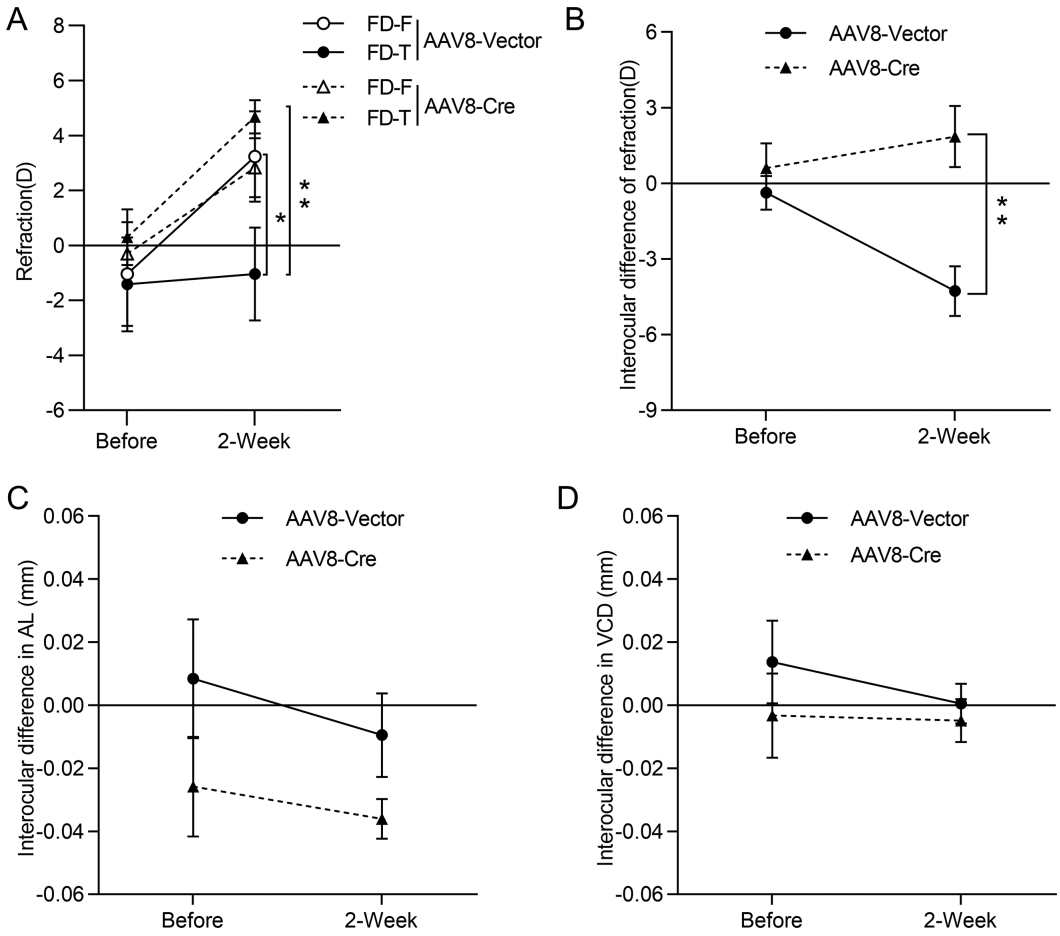

Figure 10. Scleral HIF-2α knockdown inhibits myopia development. (**A**) Refraction of FD-T and FD-F eyes in the AAV8-vector and AAC8-Cre groups after 2 weeks of FD. (**B-D**) Interocular differences (FD-T eye minus FD-F eye) in refraction (**B**), AL (**C**), and VCD (**D**), before and after 2 weeks of FD. Data are expressed as means ± SEM; $n = 7$ and 13 for AAV8-vector and AAV8-Cre mice respectively. *$P < 0.05$; **$P < 0.01$; 2-way RM-ANOVA, original FDR method of Benjamini and Hochberg (**A**) or Bonferroni's post hoc tests (**B–D**). D, diopter.

an in vivo scleral HIF-1α/HIF-2α knockdown model and an in vitro scleral fibroblast HIF-1α/HIF-2α knockdown model were used to document that HIF-2α rather than HIF-1α mediated scleral hypoxia induced MMP-2 upregulation in fibroblasts. However, it is unclear whether scleral hypoxia contributes to MMP-2 upregulation in macrophages. Tissue-specific patterns of induction of HIF-1α or/and HIF-2α inducing upregulation of diverse transcriptional target genes may elicit control through overlapping and/or distinct roles in numerous biological processes.[32] Moreover, the involvement of HIF-1α or/and HIF-2α in mediating hypoxia induced activation of downstream events may not be the same in different cell types, even within the same tissue.[33] Therefore, establishing fibroblast and macrophage-specific HIF-1α and HIF-2α deletion models might be necessary to characterize the cell-specific HIF-1/2α regulatory effects on myopia development in future studies.

During myopia development, the decrease in scleral collagen accumulation is due to the combined effects of decelerated synthesis and accelerated degradation.[5] The current study demonstrates that scleral HIF-2α has an important role in mediating control of MMP-2 upregulation and collagen degradation in myopia progression. Scleral HIF-1α knockdown suppressed the FD-induced declines in collagen accumulation without altering the MMP-2 upregulation. These data indicate that scleral HIF-1α likely contributes to collagen remodeling and myopia development by either inhibiting collagen synthesis or upregulating other subtypes of proteases augmenting collagen degradation. These results suggest that both HIF-1α and HIF-2α likely have unique roles in inducing scleral ECM remodeling and in turn myopia progression. Nevertheless, our studies just provide preliminary clues regarding the scleral mechanism underlying hypoxia-induced myopia. To fully elucidate the unique and overlapping functions of HIF-1α and HIF-2α in normal refractive development and myopia development, a comparative RNA-sequencing, proteomic, or metabolomic mapping procedure is needed. Besides HIF-1α and HIF-2α, HIF-3α is also an important oxygen-dependent transcription factor mediating the hypoxic response.[34,35] They share the same HIF-1β heterodimer, also known as ARNT, to form a transcriptionally active complex.[35] The possible involvement of HIF-3α in the scleral ECM remodeling during myopia development needs further study. In future studies, a scleral HIF-1β knockdown model might be required to more fully explore its overall function in mediating hypoxia control of myopia development.

We acknowledge several limitations of our study. First, myopic shift in refraction does not correlate well with the

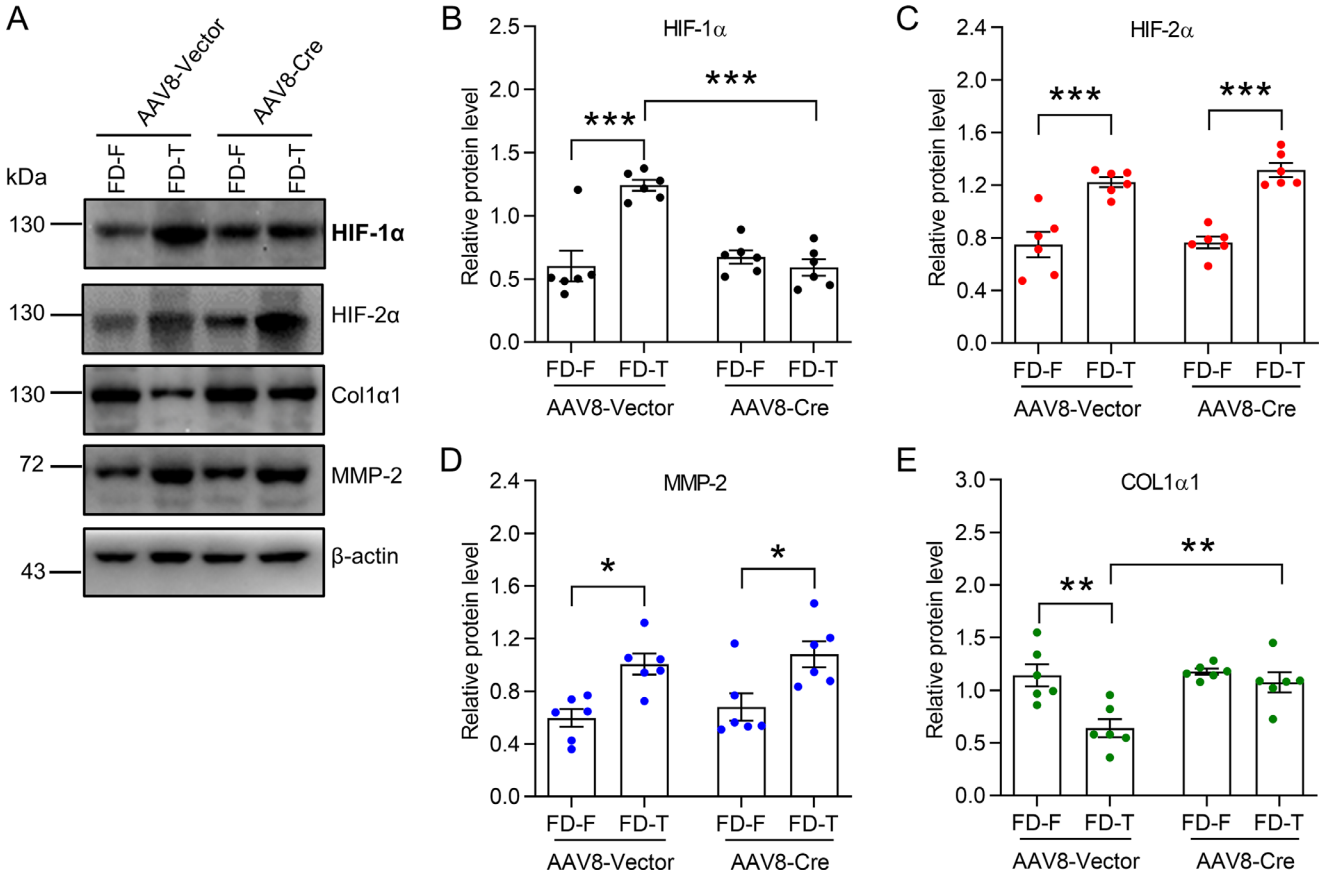

Figure 11. Western blot analyses of FD-treated scleral HIF-1α knockdown mice. Sub-Tenon's space in the right eye of *Hif-1α*$^{fl/fl}$ mice were injected with AAV8-vector or AAV8-Cre. After 1 week, myopia was induced for 2 additional weeks in the right eye (FD-T), whereas the left eye served as non-FD fellow-eye control (FD-F). (**A**) Protein levels of scleral HIF-1α, HIF-2α, MMP-2, and COL1α1 after 2 weeks of myopia induction; β-actin was used as the loading control. (**B-E**) Densitometric quantification of Western blot results of HIF-1α (**B**), HIF-2α (**C**), MMP-2 (**D**), and COL1α1 (**E**), respectively ($n = 6$). Each data point represents an independent mouse. Data in **B** to **E** represent the means ± SEM. *$P < 0.05$; **$P < 0.01$; ***$P < 0.001$; 2-way ANOVA with Bonferroni's post hoc tests.

elongation of AL and VCD in the current study (see Figs. 8A–D). This similar lack of correlation was described in our previous studies.[36,37] This negative result agrees with the reported results studies of other groups.[38,39] One possible explanation for this lack of agreement is that the current OCT instrumentation has only limited repeatability and poor resolution to obtain accurate and reproducible axial measurements of the small mouse eyes. Their AL is only about 3.3 mm, which is one of the major hindrances of using the mouse model.[40] Establishment of an improved OCT system with higher resolution and greater accuracy may overcome this hindrance in future studies. Second, the current study did not investigate the role of HIF-1α in down-regulating collagen expression during myopia development. However, several different studies have reported HIF-1α to be involved in mediating collagen expression by inhibiting COL1A1 transcription in human fibroblasts.[30,31] Nevertheless, further studies are still needed to determine the role for HIF-1α in regulating scleral COL1α1 expression during myopia development. Third, the latent rather than the active form of MMP-2 underwent upregulation in the current study. This increase does not necessarily reflect a corresponding increase in MMP-2 activity. The amount of the active form of MMP-2 was low in the sclera (see Figs. 2A, 9A, 11A) such that it did not reach the level that is resolvable using densitometric quantification of Western blot results. In future studies, an in situ zymography assay or a zymography assay of the total protein of homogenized scleral tissue should be used to assess the level of scleral MMP-2 activation. MMP-2 is synthesized and secreted into the extracellular space as an inactive latent form, which is then activated by enzymatic cleavage. Accordingly, for the in vitro study, inclusion of a zymography assay of a supernatant of the culture medium of hypoxia-treated human scleral fibroblasts (see Figs. 3A, 4A, 5A) might be more informative in future studies.

Collectively, this work describes a novel role for HIF-2α as a critical regulator of scleral ECM remodeling. Hypoxia upregulates HIF-2α expression, which in turn promotes COL1α1 degradation through upregulating MMP-2 expression level. The resulting declines in COL1α1 content underlie the ECM re-organization that accompanies axial elongation. The current study highlights scleral HIF-2α as a potential target to improve therapeutic management of myopia in a clinical setting.

Acknowledgments

The authors thank Peter S. Reinach (Wenzhou Medical University, Wenzhou, China), and Nethrajeith Srinivasalu (University

of Newcastle, Callaghan, New South Wales, Australia) for critical comments and editorial support in manuscript preparation.

Supported by the National Natural Science Foundation of China grants 82025009 (to X.Z.), 82171097 (to F.Z.), 81830027 (to J.Q.), 81700868 (to F.Z.), U20A20364 (to J.Q.), and 81670886 (to X.Z.); Natural Science Foundation of Zhejiang Province (Zhejiang Provincial Natural Science Foundation) grant LQ16H120006 (to F.Z.); Scientific Bureau of Wenzhou City grant H2020007(to F.Z.); and Y20180510 (to Y.Z.).

Disclosure: **W. Wu**, None; **Y. Su**, None; **C. Hu**, None; **H. Tao**, None; **Y. Jiang**, None; **G. Zhu**, None; **J. Zhu**, None; **Y. Zhai**, None; **J. Qu**, None; **X. Zhou**, None; **F. Zhao**, None

References

1. Morgan IG, Ohno-Matsui K, Saw SM. Myopia. *Lancet (London, England)*. 2012;379:1739–1748.
2. Morgan IG, Wu PC, Ostrin LA, et al. IMI Risk Factors for Myopia. *Invest Ophthalmol Vis Sci*. 2021;62:3.
3. Holden BA, Fricke TR, Wilson DA, et al. Global Prevalence of Myopia and High Myopia and Temporal Trends from 2000 through 2050. *Ophthalmology*. 2016;123:1036–1042.
4. Ikuno Y. Overview of the complications of high myopia. *Retina (Philadelphia, Pa)*. 2017;37:2347–2351.
5. McBrien NA. Regulation of scleral metabolism in myopia and the role of transforming growth factor-beta. *Exp Eye Res*. 2013;114:128–140.
6. Wallman J, Winawer J. Homeostasis of eye growth and the question of myopia. *Neuron*. 2004;43:447–468.
7. Jones BE, Thompson EW, Hodos W, Waldbillig RJ, Chader GJ. Scleral matrix metalloproteinases, serine proteinase activity and hydrational capacity are increased in myopia induced by retinal image degradation. *Exp Eye Res*. 1996;63:369–381.
8. Rada JA, Shelton S, Norton TT. The sclera and myopia. *Exp Eye Res*. 2006;82:185–200.
9. Zhao F, Zhou Q, Reinach PS, et al. Cause and Effect Relationship between Changes in Scleral Matrix Metallopeptidase-2 Expression and Myopia Development in Mice. *Am J Pathol*. 2018;188:1754–1767.
10. Zhao F, Wu H, Reinach PS, et al. Up-Regulation of Matrix Metalloproteinase-2 by Scleral Monocyte-Derived Macrophages Contributes to Myopia Development. *Am J Pathol*. 2020;190:1888–1908.
11. Wu H, Chen W, Zhao F, et al. Scleral hypoxia is a target for myopia control. *Proc Natl Acad Sci USA*. 2018;115:E7091–e7100.
12. Zhao F, Zhang D, Zhou Q, et al. Scleral HIF-1α is a prominent regulatory candidate for genetic and environmental interactions in human myopia pathogenesis. *EBioMedicine*. 2020;57:102878.
13. Ben-Yosef Y, Lahat N, Shapiro S, Bitterman H, Miller A. Regulation of endothelial matrix metalloproteinase-2 by hypoxia/reoxygenation. *Circulation Res*. 2002;90:784–791.
14. Jing SW, Wang YD, Kuroda M, et al. HIF-1α contributes to hypoxia-induced invasion and metastasis of esophageal carcinoma via inhibiting E-cadherin and promoting MMP-2 expression. *Acta Medica Okayama*. 2012;66:399–407.
15. Liu Y, Zhang H, Yan L, et al. MMP-2 and MMP-9 contribute to the angiogenic effect produced by hypoxia/15-HETE in pulmonary endothelial cells. *J Molec Cell Cardiol*. 2018;121:36–50.
16. Muñoz-Nájar UM, Neurath KM, Vumbaca F, Claffey KP. Hypoxia stimulates breast carcinoma cell invasion through MT1-MMP and MMP-2 activation. *Oncogene*. 2006;25:2379–2392.
17. Ye H, Zheng Y, Ma W, et al. Hypoxia down-regulates secretion of MMP-2, MMP-9 in porcine pulmonary artery endothelial and smooth muscle cells and the role of HIF-1. *J Huazhong Univ Sci Technol Med Sci*. 2005;25:382–384, 407.
18. Riches K, Morley ME, Turner NA, et al. Chronic hypoxia inhibits MMP-2 activation and cellular invasion in human cardiac myofibroblasts. *J Molec Cell Cardiol*. 2009;47:391–399.
19. Li NA, Wang H, Zhang J, Zhao E. Knockdown of hypoxia inducible factor-2α inhibits cell invasion via the downregulation of MMP-2 expression in breast cancer cells. *Oncol Lett*. 2016;11:3743–3748.
20. Roth KJ, Copple BL. Role of Hypoxia-Inducible Factors in the Development of Liver Fibrosis. *Cell Molec Gastroenterol Hepatol*. 2015;1:589–597.
21. Semenza GL. Hypoxia-inducible factors in physiology and medicine. *Cell*. 2012;148:399–408.
22. Tong L, Cui D, Zeng J. Topical bendazol inhibits experimental myopia progression and decreases the ocular accumulation of HIF-1α protein in young rabbits. *Ophthalmic Physiological Optics*. 2020;40:567–576.
23. Schaeffel F, Burkhardt E, Howland HC, Williams RW. Measurement of refractive state and deprivation myopia in two strains of mice. *Optom Vis Sci*. 2004;81:99–110.
24. Zhou X, Shen M, Xie J, et al. The development of the refractive status and ocular growth in C57BL/6 mice. *Invest Ophthalmol Vis Sci*. 2008;49:5208–5214.
25. Qu J, Zhou X, Xie R, et al. The presence of m1 to m5 receptors in human sclera: evidence of the sclera as a potential site of action for muscarinic receptor antagonists. *Current Eye Res*. 2006;31:587–597.
26. Livak KJ, Schmittgen TD. Analysis of relative gene expression data using real-time quantitative PCR and the 2(-Delta Delta C(T)) Method. *Methods (San Diego, Calif)*. 2001;25:402–408.
27. Stegen S, Laperre K, Eelen G, et al. HIF-1α metabolically controls collagen synthesis and modification in chondrocytes. *Nature*. 2019;565:511–515.
28. Bentovim L, Amarilio R, Zelzer E. HIF1α is a central regulator of collagen hydroxylation and secretion under hypoxia during bone development. *Development (Cambridge, England)*. 2012;139:4473–4483.
29. Myllyharju J, Schipani E. Extracellular matrix genes as hypoxia-inducible targets. *Cell Tissue Res*. 2010;339:19–29.
30. Duval E, Bouyoucef M, Leclercq S, Baugé C, Boumédiene K. Hypoxia inducible factor 1 alpha down-regulates type i collagen through Sp3 transcription factor in human chondrocytes. *IUBMB Life*. 2016;68:756–763.
31. Duval E, Leclercq S, Elissalde JM, Demoor M, Galéra P, Boumédiene K. Hypoxia-inducible factor 1alpha inhibits the fibroblast-like markers type I and type III collagen during hypoxia-induced chondrocyte redifferentiation: hypoxia not only induces type II collagen and aggrecan, but it also inhibits type I and type III collagen in the hypoxia-inducible factor 1alpha-dependent redifferentiation of chondrocytes. *Arthritis Rheumatism*. 2009;60:3038–3048.
32. Stroka DM, Burkhardt T, Desbaillets I, et al. HIF-1 is expressed in normoxic tissue and displays an organ-specific regulation under systemic hypoxia. *FASEB J*. 2001;15:2445–2453.
33. Wiesener MS, Jürgensen JS, Rosenberger C, et al. Widespread hypoxia-inducible expression of HIF-2alpha in distinct cell populations of different organs. *FASEB J*. 2003;17:271–273.
34. Zhang P, Yao Q, Lu L, Li Y, Chen PJ, Duan C. Hypoxia-inducible factor 3 is an oxygen-dependent transcription activator and regulates a distinct transcriptional response to hypoxia. *Cell Rep*. 2014;6:1110–1121.

35. Duan C. Hypoxia-inducible factor 3 biology: complexities and emerging themes. *Am J Physiol Cell Physiol*. 2016;310:C260–269.
36. Li Q, Zhu H, Fan M, et al. Form-deprivation myopia down-regulates calcium levels in retinal horizontal cells in mice. *Exp Eye Res*. 2022;218:109018.
37. Zhao F, Li Q, Chen W, et al. Dysfunction of VIPR2 leads to myopia in humans and mice. *J Med Genetics*. 2022;59:88–100.
38. Landis EG, Chrenek MA, Chakraborty R, et al. Increased endogenous dopamine prevents myopia in mice. *Exp Eye Res*. 2020;193:107956.
39. Bergen MA, Park HN, Chakraborty R, et al. Altered Refractive Development in Mice With Reduced Levels of Retinal Dopamine. *Invest Ophthalmol Vis Sci*. 2016;57:4412–4419.
40. Schaeffel F, Feldkaemper M. Animal models in myopia research. *Clin Exp Optom*. 2015;98:507–517.

Investigative Ophthalmology & Visual Science